Microbiol. **40**: 1826–1830.
18) Sugita, T., Takashima, M., Kodama, M., Tsuboi, R., and Nishikawa, A. 2003. Description of a new yeast species, *Malassezia japonica*, and its detection in patients with atopic dermatitis and healthy subjects. J. Clin. Microbiol. **41**: 4695–4699.
19) Sugita, T., Kodama, M., Saito, M., Ito, T., Kato, Y., Tsuboi, R., and Nishikawa, A. 2003. Sequence diversity of the intergenic spacer region of the rRNA gene of *Malassezia globosa* colonizing the skin of patients with atopic dermatitis and healthy individuals. J. Clin. Microbiol. **41**: 3022–3027.
20) Thompson, J.D., Higgins, D.G., and Gibson, T.J. 1994. CLUSTAL W: improving the sensitivity of progressive multiple sequence alignment through sequence weighting, position-specific gap penalties and weight matrix choice. Nucleic Acids Res. **22**: 4673–4680.
21) Werfel, T., and Kapp, A. 1998. Environmental and other major provocation factors in atopic dermatitis. Allergy **53**: 731–739.
22) Wessels, M.W., Doekes, G., Van Ieperen-Van Kijk, A.G., Koers, W.J., and Young, E. 1991. IgE antibodies to *Pityrosporum ovale* in atopic dermatitis. Br. J. Dermatol. **125**: 227–232.
23) Xu, J., Ramos, A.R., Vilgalys, R., and Mitchell, T.G. 2000. Clonal and spontaneous origins of fluconazole resistance in *Candida albicans*. J. Clin. Microbiol. **38**: 1214–1220.
24) Yamamoto, A., Serizawa, S., Ito, M., and Sato, Y. 1991. Stratum corneum lipid abnormalities in atopic dermatitis. Arch. Dermatol. Res. **283**: 219–223.

Microbiol. Immunol., 48(8), 579–583, 2004

A New Yeast, *Malassezia yamatoensis*, Isolated from a Patient with Seborrheic Dermatitis, and Its Distribution in Patients and Healthy Subjects

Takashi Sugita*[,1], Mami Tajima[2], Masako Takashima[3], Misato Amaya[2], Masuyoshi Saito[2], Ryoji Tsuboi[2], and Akemi Nishikawa[4]

[1]*Department of Microbiology and* [4]*Department of Immunobiology, Meiji Pharmaceutical University, Kiyose, Tokyo 204–8588, Japan,* [2]*Department of Dermatology, Tokyo Medical University, Shinjuku-ku, Tokyo 160–0023, Japan, and* [3]*Japan Collection of Microorganisms, RIKEN (The Institute of Physical and Chemical Research), Wako, Saitama 351–0198, Japan*

Received March 22, 2004; in revised form, May 7, 2004. Accepted May 14, 2004

Abstract: **Over the last few years, new *Malassezia* species have been found regularly in Japanese subjects. We isolated another new *Malassezia* species from a Japanese patient with seborrheic dermatitis (SD), and named it *M. yamatoensis*. In its physiological characteristics and the utilization of Tween by *M. yamatoensis* is similar to that of *M. furfur* and *M. dermatis*. It is distinguished by its growth temperature. To examine the distribution of the microorganism in the skin of patients with SD and atopic dermatitis (AD), and healthy subjects, we applied transparent dressings to the skin, and detected *M. yamatoensis* DNA using a non-culture-based method that consisted of nested PCR with specific primers. *M. yamatoensis* DNA was detected from 3 of 31 SD patients (9.7%), 5 of 36 AD patients (13.9%), and 1 of 22 healthy subjects (4.6%). Therefore, *M. yamatoensis* is a rare member of the cutaneous microflora.**

Key words: ***Malassezia yamatoensis*, New species, Seborrheic dermatitis, Microflora**

With the exception of *Malassezia pachydermatis*, *Malassezia* species require a lipid for growth, and are part of the human cutaneous microflora. In dermatology, *Malassezia* species are important fungi clinically, as they are associated with pityriasis versicolor, seborrheic dermatitis (SD), *Malassezia* folliculitis, and atopic dermatitis (AD) (2–4). Although *M. furfur* was previously thought to be the causative agent or trigger factor in all of these skin diseases, Guého et al. (6) reclassified this microorganism into several species in 1996. Based on the new taxonomy of the genus *Malassezia*, several studies have examined the relationship between the newly defined species and skin diseases (1, 7, 8, 12). Our research group has also analyzed the cutaneous microflora of AD patients and healthy subjects using a molecular-based non-culture method (17, 19). During these studies, we isolated two new *Malassezia* species from Japanese AD patients and healthy subjects: *M. dermatis* (18) and *M. japonica* (20). Subsequently, we analyzed the cutaneous microflora of SD patients and found an additional new *Malassezia* species. In this paper, we propose a new species, *M. yamatoensis*, and describe the distribution of this microorganism in the skin of SD and AD patients, and healthy subjects.

**Address correspondence to* Dr. Takashi Sugita, Department of Microbiology, Meiji Pharmaceutical University, 2–522–1 Noshio, Kiyose, Tokyo 204–8588, Japan. Fax: +81–424–95–8762. E-mail: sugita@my-pharm.ac.jp

Materials and Methods

Strains. Two *Malassezia* strains (M 9985 and M 9986) were isolated from a lesion on the wing of the nose of a 30-year-old male SD patient. OpSite transparent dressings (Smith and Nephew Medical, Ltd., Hull, U.K.) were applied to the skin of the SD patient and then transferred onto modified Leeming and Notman agar (10 g glucose, 10 g peptone, 8 g bile salts (OXOID, Hampshire, U.K.), 2 g yeast extract, 0.5 g glycerol monostearate, 15 g agar, 10 ml glycerol, 5 ml Tween 60, 20 ml olive oil, and 50 mg chloramphenicol (Sankyo, Tokyo) per liter) as recommended by the Centraalbureau voor Schimmelcultures, and incubated at 32 C.

rDNA sequencing and phylogenetic analysis. In the rRNA gene, D1/D2 26S rDNA, the internal transcribed spacer (ITS) region including 5.8S rDNA, and inter-

Abbreviations: AD, atopic dermatitis; SD, seborrheic dermatitis.

genic spacer (IGS) 1 region were sequenced directly from PCR products using the primer pairs NL-1 (5'-GCATATCAATAAGCGGAGGAAAAG) and NL-4 (5'-GGTCCGTGTTTCAAGACGG) (11), pITS-F (5'-GTCGTAACAAGGTTAACCTGCGG) and pITS-R (5'-TCCTCCGCTTATTGATATGC) (16), and 26SBF (5'-AGCTGCTGCCAATGCTAGCTC) and Mala-R (5'-TACTGCTGTGAATGCTCCAGC) (20), respectively. The PCR products were sequenced using an ABI 310 DNA sequencer and a BigDye Terminator Cycle Sequencing Ready Reaction kit (Perkin-Elmer Applied Biosystems, Calif., U.S.A.) according to the manufacturer's instructions. The sequences were aligned using Clustal W software (21). For a neighbor-joining analysis (15), the distances between sequences were calculated using Kimura's two-parameter model (10). A bootstrap analysis was conducted with 100 replications (5).

Taxonomic characteristics. Tween 20, 40, 60, and 80 utilization, catalase reactions, and diazonium blue B (DBB) reactions were performed, as described by Guého et al. (6). The morphology was examined on modified Leeming and Notman agar (LNA) after incubation at 32 C for 7 days. Ubiquinone molecules were identified using the method of Nakase and Suzuki (13).

Direct DNA detection in samples from patients with atopic dermatitis, seborrheic dermatitis, and healthy subjects.

i) Subjects. To examine the distribution of *M. yamatoensis* on the skin of patients and healthy subjects, 31 SD outpatients (25 males, 6 females; aged from 20 to 79, mean 48.2±18.6 years) and 36 AD outpatients (24 males, 12 females; aged from 20 to 64, mean 33.3±10.5 years) at Tokyo Medical University Hospital and 22 healthy students (7 males, 15 females; aged from 19 to 25, mean 20.7±1.6 years old) at Meiji Pharmaceutical University were involved in this study. Written informed consent was obtained from each subject.

ii) Design of M. yamatoensis *species-specific primers for PCR.* From the sequence of the IGS1 region, *M. yamatoensis*-specific primers were designed: Yama-IGS1F (5'-CGATCAAACTTCTCTGTGTCCAG) and Yama-IGS1R (5'-TGTGTGGGAGGTAGAAGAGGCA). The primers' specificity was confirmed using the strains of *M. yamatoensis* and known *Malassezia* species (*M. dermatis, M. furfur, M. globosa, M. japonica, M. obtusa, M. pachydermatis, M. restricta, M. slooffiae*, and *M. sympodialis*) as shown in Table 1.

Table 1. Specificity of the primers for *Malassezia yamatoensis* and related species

Species	Strain	Specificity	
		26SBF and Mala-R	Yama-IGS1F and Yama-IGS1R
Malassezia yamatoensis sp. nov.	M 9985	+	+
	M 9986	+	+
Malassezia dermatis	M 9927	−	−
	M 9929	−	−
Malassezia furfur	CBS 4162	+	−
	CBS 6000	+	−
	CBS 7982	+	−
Malassezia globosa	CBS 7966	+	−
	M 9972	+	−
Malassezia japonica	M 9966	+	−
	M 9967	+	−
Malassezia obtusa	CBS 7876	+	−
	Clinical isolate 2-17	+	−
Malassezia pachydermatis	CBS 1879	+	−
Malassezia restricta	CBS 7991	+	−
	M 9976	+	−
Malassezia slooffiae	CBS 7956	+	−
	M 9980	+	−
Malassezia sympodialis	CBS 7222	−	−
	M 9978	−	−
Candida albicans	CBS 562	−	−
Candida guilliermondii	CBS 566	−	−
Candida parapsilosis	CBS 604	−	−
Rhodotorula mucilaginosa	CBS 17	−	−

CBS, Centraal Bureau voor Schimmelcultures, Baarn, The Netherlands; M, Meiji Pharmaceutical University, Tokyo, Japan.

+, positive reaction; −, negative reaction.

iii) Analysis of the M. yamatoensis *microflora.* *Malassezia* DNA was extracted from the OpSite dressings using a previously described method (17). The DNA (3 μl) extracted from each sample was added to 47 μl of the PCR master mixture. PCR was performed with an initial denaturation at 94 C for 3 min, followed by 30 cycles of 30 sec at 94 C, 1 min at 57 C, and 30 sec at 72 C, and a final extension at 72 C for 10 min with primers 28SBF and Mala-R. In the nested PCR step, 1 μl of the first amplification product was added to a new reaction mixture. The PCR consisted of an initial denaturation at 94 C for 3 min, followed by 30 cycles of 30 sec at 94 C, 1 min at 59 C, and 15 sec at 72 C, and a final extension at 72 C for 10 min with primers Yama-IGS1F and Yama-IGS1R. We confirmed the absence of false positive reactions by determining the DNA sequences of the PCR products after cloning them in pCR2.1 vector (Invitrogen), since various species, including bacteria and filamentous fungi, colonize the skin surface.

Results and Discussion

M. yamatoensis clustered with *M. furfur, M. obtusa,* and *M. japonica* with 93% bootstrap support on trees constructed using the D1/D2 26S rDNA (Fig. 1). The dissimilarity between the D1/D2 26S rRNA gene of the isolates and these three phylogenetically close species exceeded 4.6%. The DNA sequence of the ITS region of *M. yamatoensis* differs by approximately 40%. The divergence between *M. yamatoensis* and known *Malassezia* species is sufficient to resolve them as individual species (14, 16). The nucleotide sequences (D1/D2 26S rDNA, ITS, and IGS regions) determined in this study have been deposited with the DNA Data Bank of Japan (DDBJ), as AB125261 to AB125266. The physiological characteristics of *M. yamatoensis* and other *Malassezia* species are shown in Table 2. The characteristics of *M. yamatoensis* are similar to those of *M. dermatis* and *M. furfur*, but *M. yamatoensis* cannot

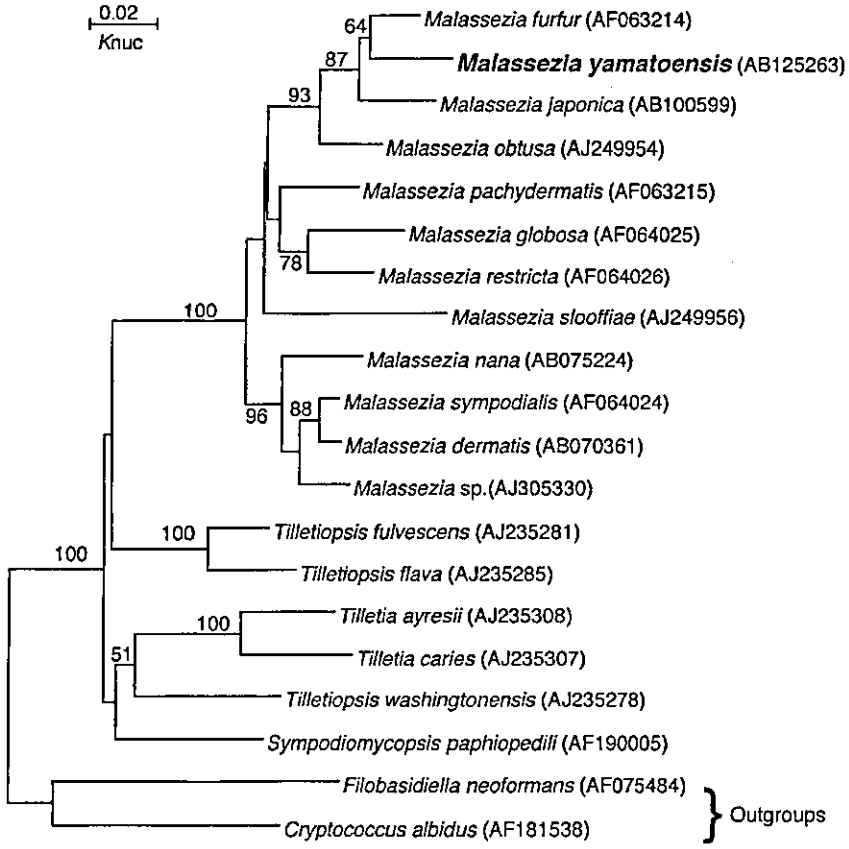

Fig. 1. Phylogenetic trees constructed using the D1/D2 26S rDNA sequences of *M. yamatoensis* and related Ustilaginomycetes species. The DDBJ/GenBank accession numbers are indicated in parentheses. The numerals are the confidence level from 100 replicate bootstrap samplings (frequencies less than 50% are not indicated). *K*nuc, Kimura's parameter (10).

Table 2. Physiological characteristics of *Malassezia yamatoensis* and other *Malassezia* species

Species	Growth on SDA[a] at 32 C	Growth on mDixon[b] at			Catalase reaction	Utilization of			
		32 C	37 C	40 C		10% Tween 20	0.5% Tween 40	0.5% Tween 60	0.1% Tween 80
Malassezia yamatoensis	−	+	+	−	+	+	+	+	+
Malassezia dermatis[a]	−	+	+	+	+	+	+	+	+
Malassezia sympodialis[b]	−	+	+	+	+	−	+	+	+
Malassezia furfur[b]	−	+	+	+	+	+	+	+	+
Malassezia nana[c]	−	+	+	+/−	+	+/−	+	+	±
Malassezia slooffiae[b]	−	+	+	+	+	± or +	+	+	−
Malassezia japonica[d]	−	+	+	−	+	−	±	+	−
Malassezia globosa[b]	−	+	± or −	−	+	−	−	−	−
Malassezia obtusa[b]	−	+	± or +	−	+	−	−	−	−
Malassezia restricta[b]	−	+	+	−	−	−	−	−	−
Malassezia pachydermatis[b]	+	+	+	+	± or +	−	+	+	+

[a] Sugita et al. (18).
[b] Guého et al. (6).
[c] Hirai et al. (9).
[d] Sugita et al. (20).
[e] Sabouraud dextrose agar.
[f] modified Dixon agar.
+, positive; −, negative; ±, weakly positive.

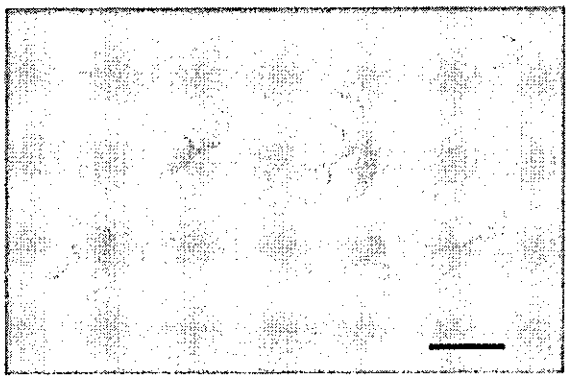

Fig. 2. Vegetative cells of *Malassezia yamatoensis* M 9985 grown in LNA for 7 days at 32 C. The scale bar indicates 10 μm.

grow at 40 C.

We analyzed 268 samples from 89 subjects (62 samples from 31 SD patients, 140 samples from 36 AD patients, 66 samples from 22 healthy subjects). *M. yamatoensis* was detected in only 3 SD patients (9.7%), 5 AD patients (13.9%), and 1 healthy subject (4.6%). As *M. yamatoensis* is a minor member of the microflora in human skin, this microorganism is thought not to be a major participant in skin disease. Since Guého et al. (6) proposed a new taxonomy of the genus *Malassezia* in 1996, four new *Malassezia* species have been found. Of these four species, *M. nana* (9) was isolated from animals, and our research group found three (*M. dermatis* (18), *M. japonica* (20), and *M. yamatoensis* (this study)) on humans.

In conclusion, *M. yamatoensis* is a new member of the cutaneous microflora on humans, although it is not a major member of the microflora. Its taxonomic description is also stated.

Latin Diagnosis of Malassezia yamatoensis *Sugita, Takashima, Tajima, Tsuboi et Nishikawa sp. nov.*

In LNA, post dies 6 ad 32 C, cellulae vegetativae, ovoideae vel ellipsoideae (2–4.5)×(2–7.5) μm, e basi lata gemmantes. Cultura xanthoalba, semi-nitida, rugosa, interdum plicata, et butyracea et margo glabra aut lobulata. In agaro glucoso-peptonico Tween 20 (10%), 40 (0.5%), 60 (0.5%) et 80 (0.1%) addito crescit. 37 C crescit neque 40 C. H2O2 hydrolysatur. Commutatio colori per diazonium caeruleum B positiva. Ubiquinonum majus Q-9 est. Teleomorphis ignota. Typus M 9985^T isolatus ex cute seborrhea humani, Tokyo, Japonia, vii, 2003, M. Tajima et T. Sugita, conservatur in collectionibus culturarum in 'Japan Collection of Microorganisms,' Saitama, Japonia ut JCM 12262^T, item in 'Centraalbureau voor Schimmelcultures (CBS),' Utrecht, Hollandia ut CBS 9725^T sustentat.

Description of Malassezia yamatoensis *Sugita, Takashima, Tajima, Tsuboi et Nishikawa sp. nov.*

On LNA, after 6 days at 32 C, the vegetative cells are oval to ellipsoidal (2–4.5)×(2–7.5) μm with buds formed on the narrow base. The colony is yellowish white, semi-shining, wrinkled or sometimes folded, and butyrous, and has an entire lobed margin. Growth occurs on glucose/peptone agar supplemented with Tween 20 (10%), 40 (0.5%), 60 (0.5%) and 80 (0.1%) as sole source of lipid. Good growth occurs at 37 C but

not 40 C. Catalase reaction is positive. The diazonium blue B reaction was positive. The major ubiquinone is Q-9. Teleomorph is unknown.

The type strain M 9985^T, isolated from skin of a Japanese patient with seborrheic dermatitis in Tokyo, Japan, by M. Tajima and T. Sugita in July, 2003, is maintained in the Japan Collection of Microorganisms (JCM), Saitama, Japan as JCM 12262^T, and the Centraalbureau voor Schimmelcultures (CBS), Utrecht, The Netherlands as CBS 9725^T. The other strain, M 9986 has also been deposited in the JCM and CBS, as JCM 12263 and CBS 9726, respectively.

Etymology. From Yamato, the old name of Japan where the type strain of this species was obtained.

This study was supported in part by a Grant-in-Aid for the Promotion of the Advancement of Education and Research in Graduate Schools from the Ministry of Education, Culture, Sports, Science and Technology, Japan, and a Grant-in-Aid for Scientific Research (B) from the Japan Society for the Promotion of Science.

References

1) Aspiroz, C., Ara, M., Varea, M., Rezusta, A., and Rubio, C. 2002. Isolation of *Malassezia globosa* and *M. sympodialis* from patients with pityriasis versicolor in Spain. Mycopathologia **154**: 111–117.
2) Ashbee, H.R., and Evans, E.G. 2002. Immunology of diseases associated with *Malassezia* species. Clin. Microbiol. Rev. **15**: 21–57.
3) Faergemann, J. 1998. The role of *Malassezia* species in the ecology of human skin and as pathogens. Med. Mycol. **36** (Suppl 1): 220–229.
4) Faergemann, J. 2002. Atopic dermatitis and fungi. Clin. Microbiol. Rev. **15**: 545–563.
5) Felsenstein, J. 1985. Confidence limits on phylogenies: an approach using the bootstrap. Evolution **39**: 783–791.
6) Guého, E., Midgley, G., and Guillot, J. 1996. The genus *Malassezia* with description of four new species. Antonie Leeuwenhoek **69**: 337–355.
7) Gupta, A.K., Kohli, Y., Faergemann, J., and Summerbell, R.C. 2001. Epidemiology of *Malassezia* yeasts associated with pityriasis versicolor in Ontario, Canada. Med. Mycol. **39**: 199–206.
8) Gupta, A.K., Kohli, Y., Summerbell, R.C., and Faergemann, J. 2001. Quantitative culture of *Malassezia* species from different body sites of individuals with or without dermatoses. Med. Mycol. **39**: 243–251.
9) Hirai, A., Kano, R., Makimura, K., Duarte, E.R., Hamdan, J.S., Lachance, M.A., Yamaguchi, H., and Hasegawa, A. 2003. *Malassezia nana* sp. nov., a novel lipid-dependent yeast species isolated from animals. Int. J. Syst. Evol. Microbiol. in press.
10) Kimura, M. 1980. A simple method for estimating evolutionary rate of base substitutions through comparative studies of nucleotide sequences. J. Mol. Evol. **16**: 111–120.
11) Kurtzman, C.P., and Robnett, C.J. 1997. Identification of clinically important ascomycetous yeasts based on nucleotide divergence in the 5′ end of the large-subunit (26S) ribosomal DNA gene. J. Clin. Microbiol. **35**: 1216–1223.
12) Nakabayashi, A., Sei, Y., and Guillot, J. 2000. Identification of *Malassezia* species isolated from patients with seborrhoeic dermatitis, atopic dermatitis, pityriasis versicolor and normal subjects. Med. Mycol. **38**: 337–341.
13) Nakase, T., and Suzuki, M. 1986. *Bullera megalospora*, a new species of yeast forming large ballistospores isolated from dead leaves of *Oryza sativa, Miscanthus sinensis*, and *Sasa* sp. in Japan. J. Gen. Appl. Microbiol. **32**: 225–240.
14) Peterson, S.W., and Kurtzman, C.P. 1991. Ribosomal RNA sequence divergence among sibling species of yeasts. System. Appl. Microbiol. **14**: 124–129.
15) Saitou, N., and Nei, M. 1987. The neighbor-joining method: a new method for reconstructing phylogenetic trees. Mol. Biol. Evol. **4**: 406–425.
16) Sugita, T., Nishikawa, A., Ikeda, R., and Shinoda, T. 1999. Identification of medically relevant *Trichosporon* species based on sequences of internal transcribed spacer regions and construction of a database for *Trichosporon* identification. J. Clin. Microbiol. **37**: 1985–1993.
17) Sugita, T., Suto, H., Unno, T., Tsuboi, R., Ogawa, H., Shinoda, T., and Nishikawa, A. 2001. Molecular analysis of *Malassezia* microflora on the skin of atopic dermatitis patients and healthy subjects. J. Clin. Microbiol. **39**: 3486–3490.
18) Sugita, T., Takashima, M., Shinoda, T., Suto, H., Unn, T., Tsuboi, R., Ogawa, H., and Nishikawa, A. 2002. New yeast species, *Malassezia dermatis*, isolated from patients with atopic dermatitis. J. Clin. Microbiol. **40**: 1363–1367.
19) Sugita, T., Kodama, M., Saito, M., Ito, M., Kato, Y., Tsuboi, R., and Nishikawa, A. 2003. Sequence diversity of the intergenic spacer region of the rRNA gene of *Malassezia globosa* colonizing the skin of patients with atopic dermatitis and healthy individuals. J. Clin. Microbiol. **41**: 3022–3027.
20) Sugita, T., Takashima, M., Kodama, M., Tsuboi, R., and Nishikawa, A. 2003. Description of a new yeast species, *Malassezia japonica*, and its detection in patients with atopic dermatitis and healthy subjects. J. Clin. Microbiol. **41**: 4695–4699.
21) Thompson, J.D., Higgins, D.G., and Gibson, T.J. 1994. CLUSTAL W: improving the sensitivity of progressive multiple sequence alignment through sequence weighting, position-specific gap penalties and weight matrix choice. Nucleic Acids Res. **22**: 4673–4680.

Original Paper

nephron
Experimental
Nephrology

Nephron Exp Nephrol 2004;98:e100–e108
DOI: 10.1159/000080685

Received: November 25, 2003
Accepted: June 11, 2004

Activation of the Smad Pathway in Glomeruli from a Spontaneously Diabetic Rat Model, OLETF Rats

Yoko Furuse[a] Naotake Hashimoto[c] Mamiko Maekawa[b] Yoshiro Toyama[b]
Atsuhito Nakao[d] Itsuo Iwamoto[a] Kenichi Sakurai[a] Yoshifumi Suzuki[e]
Kazuo Yagui[a] Shigeki Yuasa[f] Kiyotaka Toshimori[b] Yasushi Saito[a]

Departments of [a]Clinical Cell Biology and [b]Anatomy and Developmental Biology, Graduate School of Medicine, Chiba University, Chiba; [c]Department of Diabetes and Metabolic Disease, Asahi General Hospital, Asahi, Chiba; [d]Department of Immunology, University of Yamanashi Faculty of Medicine, Yamanashi; [e]Department of Internal Medicine, Matsudo General Hospital, Matsudo, Chiba, and [f]Department of Ultrastructural Research, National Institute of Neuroscience, National Center of Neurology and Psychiatry, Tokyo, Japan

Key Words
Smads · Transforming growth factor-β · OLETF · Diabetic nephropathy · Glomerulus

Abstract
Background/Aims: Transforming growth factor-β (TGF-β) mediates the excess accumulation of extracellular matrix in the diabetic kidney. Smad family proteins have been identified as signal transducers for the TGF-β superfamily. We sought to characterize the role of Smad proteins in mediating TGF-β responses in the development of diabetic nephropathy. ***Methods:*** We evaluated the time course of TGF-β_1 fibronectin, Smad2 and Smad3 protein expression and Smad3 activation in glomeruli from spontaneously diabetic Otsuka Long-Evans Tokushima Fatty (OLETF) rats, using immunohistochemistry and Western blot analysis. ***Results:*** The glomeruli of diabetic OLETF rats showed not only accelerated activation of Smad3, but also enhanced protein expression of Smad2 and Smad3, which occurred in parallel to the increased expression of TGF-β and fibronectin compared with glomeruli of control, Long-Evans Tokushima Otsuka (LETO) rats at 30 weeks of age. No differences were found in TGF-β_1 fibronectin, Smad2 and Smad3 protein expression and Smad3 activation in glomeruli between the two strains at 12 weeks of age when OLETF rats were not diabetic. ***Conclusions:*** The enhancement of Smad protein expression and activation may be involved in the TGF-β signaling cascade that plays an important role in the development of diabetic nephropathy through progressive expansion of the mesangial matrix.

Introduction

Diabetic glomerulopathy is characterized by progressive expansion of the mesangial matrix without evidence of increased mesangial cell proliferation [1, 2]. Many studies have implicated the involvement of transforming growth factor-β (TGF-β) in various human renal diseases

KARGER
Fax + 41 61 306 12 34
E-Mail karger@karger.ch
www.karger.com

1660–2129/04/0983–0100$21.00/0

Accessible online at:
www.karger.com/nee

Naotake Hashimoto, MD
Department of Diabetes and Metabolic Disease, Asahi General Hospital
I-1326, Asahi, Chiba 289-2511 (Japan)
Tel. +81 479 638111, Fax +81 479 638580
E-Mail naohasi@hospital.asahi.chiba.jp

that are characterized by the accumulation of extracellular matrix including diabetic nephropathy [3–6]. In vitro, high glucose concentrations increase TGF-β expression and matrix synthesis in renal cells [7–9]. It has been demonstrated that a neutralizing antibody against TGF-β and a TGF-β antisense oligonucleotide can reduce the high glucose-induced increase in collagen or fibronectin production by mesangial cells [10, 11]. Paracrine-produced TGF-β induces accumulation of the glomerular extracellular matrix in the renal tissue of transgenic mice [12]. These lines of evidence prove that autocrine and paracrine effects of activated TGF-β play a crucial role in the progression of diabetic nephropathy.

The Smad protein family has been identified as an essential component of the intracellular signaling system for TGF-β. Smad2 and Smad3 show a high degree of structural homology and mediate signaling by TGF-β. The receptor complex activated by TGF-β binding phosphorylates Smad2 or Smad3 [13–16]. Smad4 forms a heteromeric complex with phosphorylated Smad2 or Smad3, and then the complex translocates to the nucleus and regulates transcriptional responses [17]. TGF-β-mediated phosphorylation of Smad2 or Smad3 is inhibited by Smad7, suggesting that its antagonistic effect is exerted at an important regulatory step [18]. Therefore, elucidation of the role of the Smad family proteins in diabetic kidneys may be important for clarifying the pathogenesis and treatment of diabetic nephropathy.

The Otsuka Long-Evans Tokushima Fatty (OLETF) rat exhibits obesity, late onset of hyperglycemia (after 18 weeks of age), hyperinsulinemia, and proteinuria. This rat has been utilized extensively as a model of type 2 diabetes mellitus [19–21]. The OLETF rat develops histological abnormalities specific to human diabetic nephropathy such as mesangial expansion and thickening of the glomerular basement membrane [20, 22].

In the present study, we examined protein expression and activation of the Smad-mediated pathway and its role as a downstream effector of TGF-β signaling in the progression of diabetic nephropathy using OLETF rats.

Materials and Methods

Animals

Male OLETF rats were utilized at the age of 12 and 30–39 weeks and age-matched male Long-Evans Tokushima Otsuka (LETO) rats served as controls. Both strains were obtained from the Tokushima Research Institute of Otsuka Pharmaceutical Co. (Tokushima, Japan). All rats were allowed free access to food and water. When rats were anesthetized, their body weight was measured and blood was obtained from the aorta. Blood glucose levels were measured by an electrode meter (Glucocard; Kyoto Daiichi, Kyoto, Japan). Serum immunoreactive insulin (IRI) was determined by a rat insulin radioimmunoassay kit (St. Charles, Mo., USA) according to the manufacturer's instructions. Urinary albumin was measured by an enzyme-linked immunosorbent assay kit (Exocell Inc., Philadelphia, Pa., USA) according to the manufacturer's instructions. Experiments were performed in compliance with the Principles of Laboratory Animal Care (NIH publ. No. 85-23, revised 1985).

Antibodies

Antibodies were purchased from the following vendors: rabbit polyclonal anti-TGF-β_1 antibody and fluorescein-conjugated antibody to rabbit IgG from Santa Cruz Biotechnology (Santa Cruz, Calif., USA); mouse monoclonal anti-Smad2 antibody from Transduction Laboratories (Lexington, Ky., USA); rabbit polyclonal anti-fibronectin antibody from Chemicon International (Temecula, Calif., USA); rabbit polyclonal anti-Smad3 antibody from Zymed Laboratories (South San Francisco, Calif., USA); fluorescein-conjugated antibody to mouse IgG from Kirkegaard & Perry Laboratories (Gaithersburg, Md., USA); horseradish peroxidase-conjugated antibody to rabbit IgG from Calbiochem (Darmstadt, Germany); horseradish peroxidase-conjugated antibody to mouse IgG from ICN Biomedicals (Irvine, Calif., USA); biotin-conjugated antibody to rabbit IgG from Vector Laboratories (Burlingame, Calif., USA).

Renal Tissue Specimens

Rats were anesthetized and fixed by transcardiac perfusion with a solution of 4% paraformaldehyde and 0.5% picric acid in phosphate-buffered saline (PBS). Kidneys were removed and immersed in the same fixative for 2 h at 4°C. Pieces of the cortex of kidneys were embedded in OCT compound (Sakura Finetechnical Co., Ltd, Tokyo, Japan) for producing cryostat sections. Some pieces of the cortices were paraffin-embedded.

Light Microscopy

Sections (5 μm thick) of the paraffin-embedded tissue were cut and deparaffinized by treatment with xylene, followed by graded ethanol. All sections were stained with periodic acid-Schiff (PAS) and counterstained with Mayer's hematoxylin to examine renal pathological changes. The specimens were examined under the light microscope.

Immunofluorescence Staining

Sections (20 μm thick) from the kidney tissue embedded in OCT compound were prepared using on a cryostat. Indirect immunofluorescence staining was carried out using fluorescein-conjugated secondary antibodies for evaluation of protein expression of TGF-β_1, fibronectin and Smad2 in glomeruli. All sections were washed in PBS to remove the OCT compound and incubated in PBS containing 10% Normal Goat Serum (NGS) (Gibco) and 0.1% Triton X-100 (Sigma Chemical Co., St. Louis, Mo., Japan) for 1 h at room temperature to block non-specific protein-binding sites. Subsequently, they were incubated with the primary antibodies (anti-TGF-β_1 antibody, at 1:50 dilution; anti-Smad2 antibody, at 1:30 dilution; or anti-fibronectin antibody, at 1:250 dilution) overnight at 4°C. After three 5-min washes in PBS, the sections were incubated with fluorescein-conjugated secondary antibody appropriate for the species of primary antibody used for 1 h at room temperature. The sections were washed with three 5-min washes in PBS and then mounted with

PermaFluor Aqueous Mounting Medium (Shandon, Pittsburgh, Pa., USA). The specimens were observed using a confocal laser scanning microscope (MRC-600, BioRad). Negative controls were performed without primary antibodies.

Glomeruli were randomly selected for a quantitative analysis in each section immunostained for TGF-β_1, fibronectin and Smad2 by the immunofluorescence method and sections of negative controls. The criterion for selection was a cross-sectional cut through or near the vascular poles. Seven to sixteen glomeruli were examined from at least 3 rats from each group. The average value of fluorescence intensity in each glomerulus was calculated by using NIH image 1.61 software (shareware from NIH, Bethesda, Md., USA). TGF-Gβ_1, fibronectin and Smad2 protein expression in the glomeruli was evaluated by the score yielded after subtracting the value for the negative controls from the value for sections immunostained for each protein.

Immunoperoxidase Staining

Immunolocalization of Smad3 was studied using an avidin-biotin complex peroxidase kit. Sections (5 μm thick) of paraffin-embedded tissue were cut. Following deparaffinization, endogenous peroxidase activity was quenched by incubating the tissue with 0.3% hydrogen peroxide in methanol for 30 min. Non-specific protein-binding sites were blocked with PBS containing 1% bovine serum albumin and 5% NGS for 30 min at room temperature. The sections were incubated overnight at 4°C with rabbit polyclonal anti-Smad3 antibody at 1:100 dilution. The same concentration of rabbit IgG was used as a negative control. After three 5-min washes with PBS, they were incubated with biotin-conjugated antibody to rabbit IgG in PBS with 1.5% NGS for 30 min at room temperature. Subsequently, the sections were incubated with ABC reagent: Vectastain Elite avidin-biotin complex peroxidase kit from Vector Laboratories according to the manufacturer's instructions. The bound peroxidase was detected by a 5-min reaction with hydrogen peroxide and 3,3'-diaminobenzidine tetrahydrochloride (Sigma Chemical Co.) as substrates. Mayer's hematoxylin was used as the counterstain.

Glomeruli were randomly selected for a quantitative analysis in each section immunostained for Smad3. Twenty to fifty glomeruli were examined from at least 3 rats from each group. We counted the number of immunostained nuclei in a glomerulus and calculated the ratio to the total number of the glomerular component cells. The number of component cells in each glomerulus was obtained by counting the hematoxylin-stained nuclei.

Western Blot Analysis

Rats were anesthetized and perfused in situ via the aorta with PBS (pH 7.4) to remove blood. The kidneys were excised, and the cortices were then cut into pieces. A plastic rod was used to pass the minced cortex through a 600-μm stainless mesh. The tissue that emerged through the mesh was then passed sequentially through 150-, 130-, 110-, and 90-μm filters. Intact glomeruli retained on the 110- or 90-μm filters were resuspended in ice-cold PBS, collected by centrifugation at 1,500 rpm for 5 min at 4°C. Specimens were >95% free of extraglomerular elements. Isolated glomeruli were homogenized in cell lysis buffer (100 m*M* sodium fluoride, 10 m*M* sodium pyrophosphate, 5 m*M* EDTA pH 8.0, 150 m*M* NaCl, 1% Triton X-100, 10 μg/ml bacitracin, 10 μg/ml pepstatin, 10 μg/ml leupeptin, 10 μg/ml chymostatin, 10 μg/ml aprotinin, 10 μg/ml antipain, and 0.3 mg/ml PMSF dissolved in 50 m*M* Hepes pH 7.6). The tissue homogenates were centrifuged at 15,000 rpm for 15 min at 4°C to pellet insoluble material. The protein concentrations of the supernatants were determined by BCA Protein Assay Reagent A (Pierce, Rockford, Ill., USA). Western blot analysis was performed according to the method reported previously [23] with some modifications. Protein samples (12 μg) were fractionated by electrophoresis in a polyacrylamide gel and transferred to a nitrocellulose membrane. The blot was probed with the primary antibody (rabbit polyclonal anti-TGF-β_1 antibody, 0.2 μg/ml, mouse monoclonal anti-Smad2 antibody, 0.5 μg/ml or rabbit polyclonal anti-Smad3 antibody, 2.5 μg/ml) and incubated with horseradish peroxidase-conjugated secondary antibody appropriate for the species of primary antibody used, and then visualized by chemiluminescence using a ECL kit (Amersham Biosciences, Bucks., UK). Western blot analysis was performed on 2–4 samples from different animals.

Statistical Analysis

All values are expressed as the mean ± SE. Statistical analysis was carried out using the Mann-Whitney U test. Differences were considered statistically significant at $p < 0.05$.

Results

Metabolic Data

The characteristics of the experimental rats are shown in table 1. The values of body weight and serum IRI were significantly greater in OLETF rats than in LETO rats at 12 weeks of age. However, no significant differences were found in blood glucose levels between the two strains. At the age of 30 and 39 weeks, blood glucose levels, body weights and values of IRI were significantly higher in OLETF rats than in LETO rats. Albuminuria was prominent in OLETF rats at these ages. There were no differences between the two strains in the ratio of kidney weight to body weight at each age experimented.

Light Microscopy

PAS and hematoxylin staining revealed a normal appearance of the renal tissue from LETO (fig. 1A) and OLETF (fig. 1B) rats at 12 weeks of age. At 30 weeks of age, a significant increase in the mesangial matrices was found in the glomerulus of OLETF rats (fig. 1D). No histological abnormalities were observed in the kidneys of age-matched LETO rats (fig. 1C).

Immunofluorescence Staining

We examined immunoreactivities for TGF-β, fibronectin and Smad2 in the glomeruli of rats aged 12 and 30 weeks. No differences were observed in the fluorescence intensity for TGF-β_1, fibronectin and Smad2 immunostaining in glomeruli between the two strains at 12 weeks of age (data not shown). At the age of 30 weeks, the TGF-β_1 immunostaining in glomeruli was more intense in OLETF rats (fig. 2B) than in LETO rats (fig. 2A). Non-

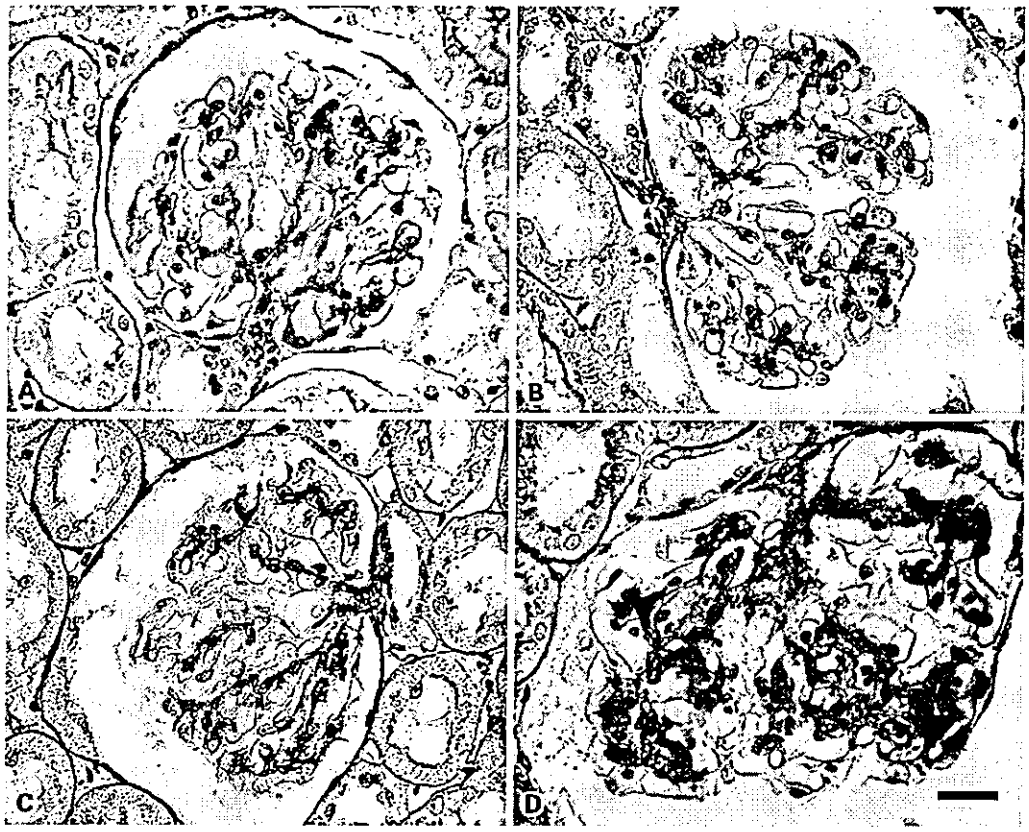

Fig. 1. Light micrographs of glomeruli from LETO (**A, C**) and OLETF (**B, D**) rats at the age of 12 weeks (**A, B**) and 30 weeks (**C, D**) stained with PAS and hematoxylin. Note the remarkable increase in the mesangial matrix in the glomerulus of OLETF rats at 30 weeks of age (**D**). Bar: 20 μm.

Table 1. Characteristics of the rats studied

	n	Body weight, g	Kidney weight, mg	Kidney weight/body weight, mg/g	Fed blood glucose mg/dl	Urinary albumin mg/dl	IRI mg/dl
12 weeks							
LETO	6	351.7±6.0	1,689±75	4.65±0.22	174.3±15.9	0.8±0.2	1.5±0.3
OLETF	5	422.0±15.0**	1,753±117	5.25±0.24	204.2±19.9	2.3±0.8	3.7±0.3**
30 weeks							
LETO	11	500.9±7.6	1,341± 84	2.98±0.17	171.0±10.2	3.9±2.6	2.7±0.9
OLETF	12	655.8±6.7***	1,831±90*	2.98±0.13	299.2±18.1**	227.9±51.5**	7.2±0.8**
39 weeks							
LETO	4	510.0±10.8	1,659±59	3.25±0.09	139.5±10.9	6.1±2.1	1.1±0.4
OLETF	3	700.0±11.5*	2,711±413*	3.40±0.11	274.7±5.0*	3,776.0±185.6*	5.0±1.7*

Data are means ± SE. * $p < 0.05$ vs. LETO; ** $p < 0.01$ vs. LETO; *** $p < 0.0001$ vs. LETO.

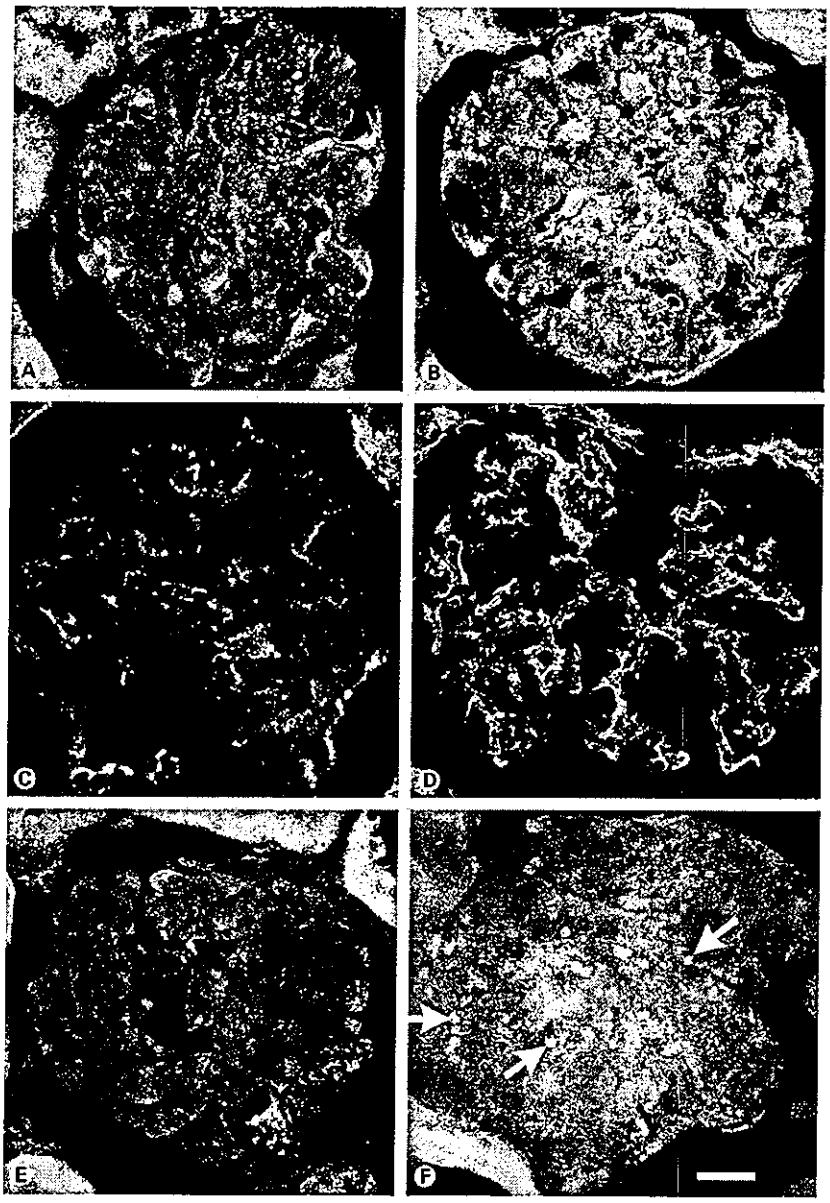

Fig. 2. Glomerular expression of TGF-β_1, fibronectin, and Smad2 proteins by immunofluorescence study. Immunofluorescence micrographs of glomeruli from LETO (**A**, **C**, **E**) and OLETF (**B**, **D**, **F**) rats at 30 weeks of age stained for TGF-β_1 (**A**, **B**), fibronectin (**C**, **D**) and Smad2 (**E**, **F**) Intense immunostaining for TGF-β_1 was found in the glomeruli from OLETF rats (**B**) compared with LETO rats (**A**). The accumulation of fibronectin was evident in the mesangial areas in OLETF rats (**D**), while much less was found in LETO rats (**C**). The immunoreactivity for Smad2 was more intense in the glomeruli of OLETF rats (**F**) than in those of LETO rats (**E**). Arrows indicate strong immunopositive reactions for Smad2 in the nuclei of the glomerular cells from OLETF rats (**F**). Bar: 20 μm.

specific staining was observed in renal tubules as previously reported by Isaka et al [24]. Intense staining for fibronectin was observed in the mesangial areas in the glomerulus of OLETF rats (fig. 2D). The staining was more striking than those of LETO rats (fig. 2C). The immunoreactivity for Smad2, which is the mediator of TGF-β signal transduction, was more intense in the glomeruli from OLETF rats compared with LETO rats (fig. 2E). Furthermore, the strong immunopositive reactions for Smad2 were found to localize in the nuclei of the glomerular cells from OLETF rats (fig. 2F). The sections stained by methods eliminating incubation with primary antibodies showed only trace staining in glomeruli (data not shown). Expression of these proteins in glomeruli was quantified as described in the Methods section. The protein expression of TGF-β_1 (fig. 3A), fibronectin (fig. 3B) and Smad2

(fig. 3C) was significantly increased in OLETF rats compared to LETO rats at 30 weeks of age.

Immunoperoxidase Staining

The immunohistochemical study for Smad3 showed that cells showing predominantly nuclear immunostaining for Smad3 were more abundant in glomeruli from OLETF rats (fig. 4D) than from LETO rats (fig. 4C) at 30 weeks of age. Positive immunostaining for Smad3 was observed in glomerular epithelial cells, mesangial cells, proximal tubular cells, and endothelial cells. Smad3 is one of the receptor-regulated Smads, which translocate from the cytoplasm into the nucleus after phosphorylation by a receptor complex activated by TGF-β stimulus. Therefore, we studied whether the Smad-mediated pathway was activated in glomeruli by calculating the ratio of cells with nuclei immunostained for Smad3 to the total component cells in a glomerulus. The glomerular cells with accelerated nuclear accumulation of Smad3 significantly increased in glomeruli from diabetic OLETF rats aged 30 weeks compared with age-matched LETO rats (fig. 5). At 12 weeks of age, Smad3 localization in the nucleus did not differ in glomeruli between both strains (fig. 4A, B, fig. 5). Incubation with rabbit IgG substituted for a primary antibody showed negative staining in renal tissue (data not shown).

Western Blot Analysis

Western blot analysis revealed that Smad2 and Smad3 in protein extracted from isolated glomeruli of OLETF rats were increased compared with control LETO rats at 30 weeks of age (fig. 6A, B). There were found more increased glomerular amounts of TGF-β_1 in OLETF rats than in LETO rats at the age of 39 weeks (fig. 6C). At 12 weeks of age, no differences were found between both rat strains (data not shown).

Discussion

In this study, we sought to elucidate whether the TGF-β/Smad signaling pathway was functional in the progression of nephropathy in OLETF rats, a genetic model of type 2 diabetes. Our results indicated that OLETF rats aged 30 and 39 weeks developed diabetes mellitus and excreted massive urinary albumin. Mesangial expansion specific to diabetic nephropathy was found in their renal tissue. Our immunofluorescence study showed that glomerular TGF-β_1 protein was increased in 30-week-old OLETF rats compared with age-matched LETO rats. This finding was consistent with the report by Yagi et al. [25].

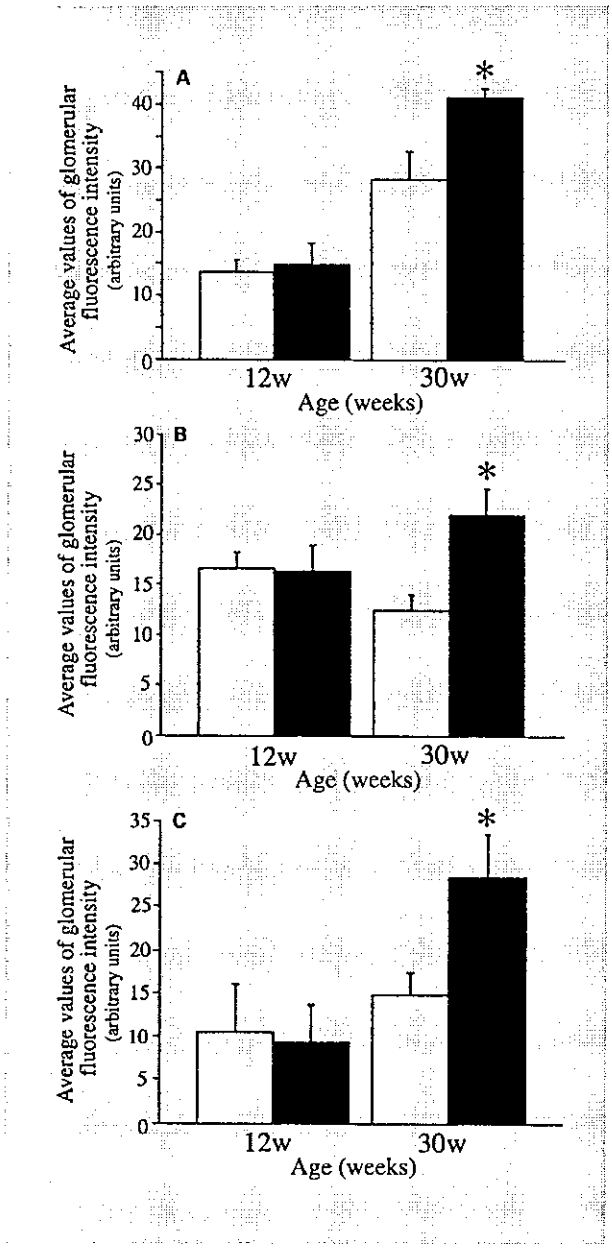

Fig. 3. Expression of TGF-β_1 (**A**), fibronectin (**B**) and Smad2 (**C**) proteins in glomeruli from OLETF (black bars) and LETO (white bars) rats was quantified as described in the Materials and Methods section. Data are summarized as mean ± SE. * $p < 0.05$ vs. LETO rats at the same age.

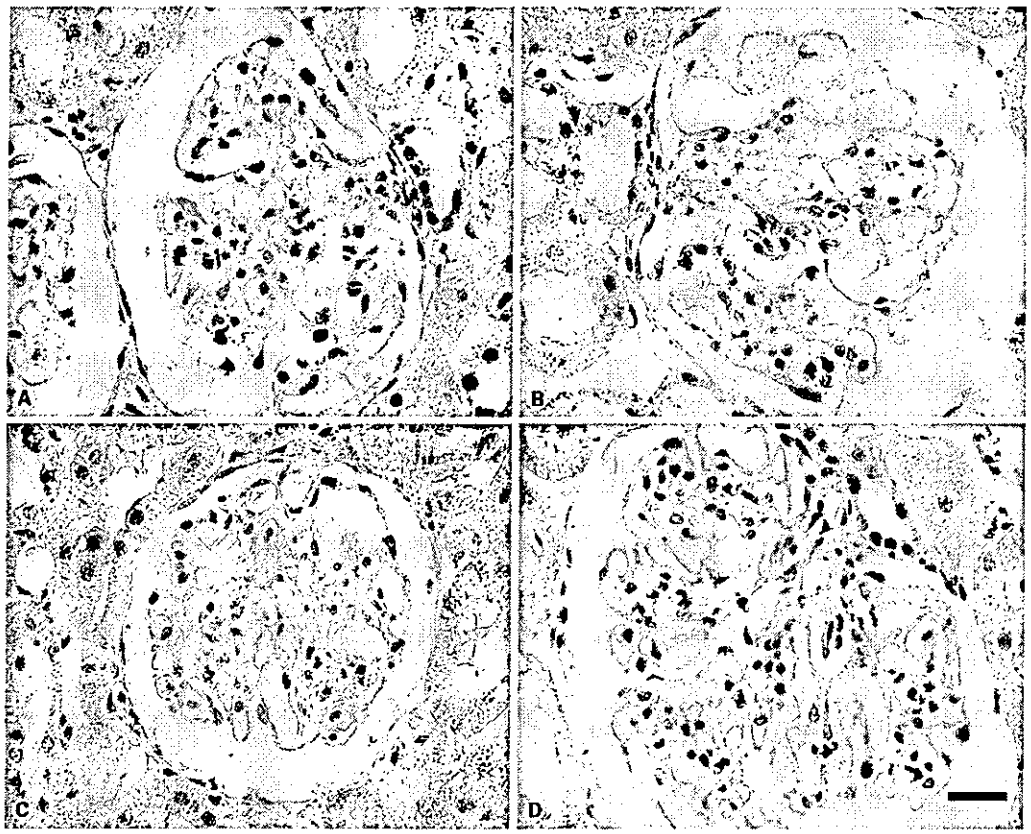

Fig. 4. Nuclear accumulation of Smad3 protein in glomeruli by immunohistochemistry. Light micrographs of glomeruli from LETO (**A**, **C**) and OLETF (**B**, **D**) rats at the age of 12 weeks (**A**, **B**) and 30 weeks (**C**, **D**) immunostained for Smad3. Note the promoted nuclear accumulation of Smad3 in glomeruli from diabetic OLETF rats at 30 weeks of age (**D**). Bar: 20 μm.

We have found increased fibronectin accumulation in the glomeruli of OLETF rats compared with LETO rats at 30 weeks of age by the immunofluorescence method. Kushiro et al. [26] reported that an increase in glomerular fibronectin was observed in 12-month-old, but not in 6-month-old OLETF rat. According to their findings and our results, glomerular fibronectin in OLETF rats was supposed to increase between about 25–30 weeks of age. The Smad pathway mediating TGF-β responses has been shown to participate in the transcriptional activation of the fibronectin gene by Isono et al. [27]. Therefore, we sought to assess the protein expression and the activation of Smad proteins in glomeruli from OLETF rats aged 30 weeks.

Indirect immunofluorescence staining showed significantly increased glomerular expression of Smad2 in diabetic OLETF rats than in LETO rats at 30 weeks of age. Moreover, Western blot analysis revealed that Smad2 and Smad3 were increased in the glomeruli of OLETF rats compared with LETO rats at the same age. Immunoperoxidase staining revealed that Smad3 localization in the nucleus was significantly increased in glomeruli of OLETF rats compared with LETO rats at this age. There were no differences in protein expression of Smad2 and Smad3 and nuclear localization of Smad3 in glomeruli between both strains at 12 weeks of age when OLETF rats were not diabetic.

These data suggest that TGF-β signaling pathway mediated by Smad proteins may be accelerated not only through TGF-β induced by high blood glucose levels but also by increased expression of Smad2 and Smad3 proteins in glomeruli from OLETF rats, and that this may

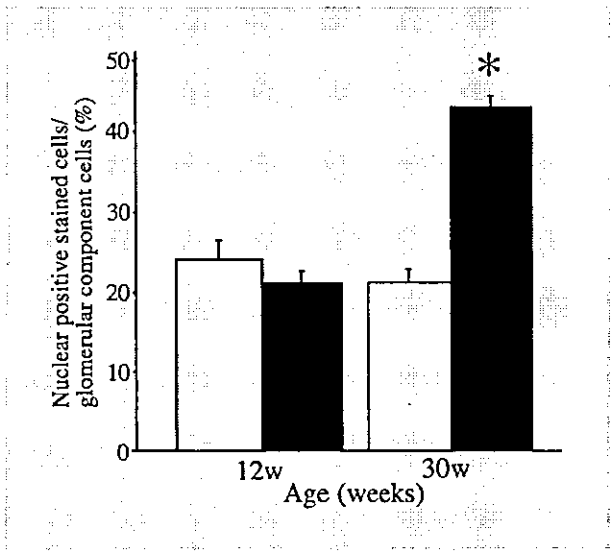

Fig. 5. Quantification of nuclear immunostain for Smad3 in glomeruli revealed significantly increased activated Smad3 in glomeruli from OLETF rats (black bars) compared to control LETO (white bars) rats at 30 weeks of age. Data are mean ± SE. * $p < 0.05$ vs. LETO rats at the same age.

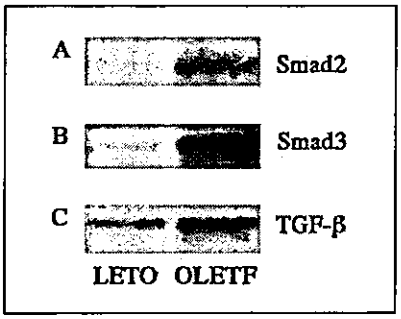

Fig. 6. Western blot analyses of glomerular proteins from OLETF and LETO rats at the age of 30 weeks with anti-Smad2 antibody (**A**) or anti-Smad3 antibody (**B**) and at the age of 39 weeks with anti-TGF-β_1 antibody (**C**). Glomerular Smad2, Smad3 and TGF-β_1, were increased in OLETF rats compared with LETO rats at 30 and 39 weeks of age when OLETF rats were diabetic.

play an important role in progression of diabetic nephropathy. Smad3 activation can be explained by the augmented expression and activation of TGF-β induced by high blood glucose concentrations in OLETF rats. Isono et al. [27] have reported that Smad3 activation was induced by TGF-β in diabetic mice kidneys, but we found not only augmented activation of Smad3 but also increased glomerular expression of Smad2 and Smad3 proteins in this spontaneously diabetic animal model. These results suggest that the total TGF-β signaling may be enormously enhanced in glomeruli of diabetic OLETF rats.

The mechanism underlying the increased expression of Smad2 and Smad3 proteins in the glomeruli of OLETF rats remains unclear. One possibility is that TGF-β itself may induce Smad protein expression. The levels of Smad2 mRNA have been observed to increase following TGF-β treatment in certain cell lines [28]. Expression of Smad7 mRNA was induced by TGF-β [18]. However, there have been no reports about the regulation of Smad3 and Smad protein production by TGF-β in the kidney or other tissues. The other possibility is that factors other than TGF-β might induce overexpression of Smad proteins in the kidney. For example, platelet-derived growth factor (PDGF) may be one such candidate. PDGF-β receptors are overexpressed in the medial smooth muscle cells from the aorta of OLETF rats before the onset of diabetes mellitus, suggesting that a genetic factor may contribute not only to atherosclerosis but also to diabetic nephropathy in these animals [29]. To that end, microalbuminuria has been reported to be clinically correlated with atherosclerosis [30–32]. The third possibility is that Smad proteins may be genetically overexpressed with increasing age in OLETF rats. However, further investigation is required for elucidation of the mechanism underlying increased expression of Smad2 and Smad3 proteins in glomeruli of OLETF rat.

In summary, we demonstrated that the Smad proteins might play an important role in the development of diabetic nephropathy in OLETF rats. Further analyses of this rat model would provide new insights into the mechanism of progression of diabetic nephropathy as well as potential treatment related to the modulation of Smad proteins.

Acknowledgment

We thank Dr. Kubosawa (Department of Pathology, Chiba Municipal Hospital, Chiba, Japan) for helpful advice.

References

1 Mauer SM, Steffes MW, Brown DM: The kidney in diabetes. Am J Med 1981;70:603–612.
2 Steffes MW, Osterby R, Chavers B, Mauer SM: Mesangial expansion as a central loss of kidney function in diabetic patients. Diabetes 1989; 38:1077–1081.
3 Bollineni JS, Raddi AS: Transforming growth factor-β_1 enhances glomerular collagen synthesis in diabetic rats. Diabetes 1993;42:1673–1677.
4 Pankewycz OG, Guan JX, Bolton WK, Gomez A, Benedict JF: Renal TGF-β regulation in spontaneously diabetic NOD mice with correlations in mesangial cells. Kidney Int 1994;46: 748–758.
5 Shankland SJ, Scholey JW, Ly H, Thai K: Expression of transforming growth factor-β_1 during diabetic renal hypertrophy. Kidney Int 1994;46:430–442.
6 Yamamoto T, Nakamura T, Noble NA, Ruoslahti E, Border WA: Expression of transforming growth factor-β is elevated in human and experimental diabetic nephropathy. Proc Natl Acad Sci USA1993;90:1814–1818.
7 Oh JH, Ha H, Yu MR, Lee HB: Sequential effects of high glucose on mesangial cell transforming growth factor-β_1 and fibronectin synthesis. Kidney Int 1998;54:1872–1878.
8 Van Det NF, Verhagen NA, Tamsma JT, Berden JH, Bruijn JA, Daha MR, van der Woude FJ: Regulation of glomerular epithelial cell production of fibronectin and transforming growth factor-β by high glucose, not by angiotensin II. Diabetes 1997;46:834–840.
9 Rocco MV, Chen Y, Goldfarb S, Ziyadeh FN: Elevated glucose stimulates TGF-β gene expression and bioactivity in proximal tubule. Kidney Int 1992;41:107–114.
10 Ziyadeh FN, Sharma K, Ericksen M, Wolf G: Stimulation of collagen gene expression and protein synthesis in murine mesangial cells by high glucose is mediated by autocrine activation of transforming growth factor-β. J Clin Invest 1994;93:536–542.
11 Kolm V, Sauer U, Olgemoller B, Schleicher ED: High glucose-induced TGF-β_1 regulates mesangial production of heparan sulfate proteoglycan. Am J Physiol 1996;270:F812–F821.
12 Wogensen L, Nielsen CB, Hjorth P, Rasmussen LM, Nielsen AH, Gross K, Sarvetnick N, Ledet T: Under control of the Ren-1c promoter, locally produced transforming growth factor-β_1 induces accumulation of glomerular extracellular matrix in transgenic mice. Diabetes 1999;48: 182–192.
13 Graff JM, Bansal A, Melton DA: Xenopus Mad proteins transduce distinct subsets of signals for the TGF-β superfamily. Cell 1996;85:479–487.
14 Heldin CH, Miyazono K, ten Dijke P: TGF-β signalling from cell membrane to nucleus through SMAD proteins. Nature 1997;390: 465–471.
15 Nakao A, Imamura T, Souchelnytskyi S, Kawabata M, Ishisaki A, Oeda E, Tamaki K, Hanai J, Heldin CH, Miyazono K, ten Dijke P: TGF-β receptor-mediated signalling through Smad2, Smad3 and Smad4. EMBO J 1997;16:5353–5362.
16 Chen Y, Bhushan A, Vale W: Smad8 mediates the signaling of the ALK-2 receptor serine kinase. Proc Natl Acad Sci USA 1997;94:12938–12943.
17 Lagna G, Hata A, Hemmati-Brivanlou A, Massague J: Partnership between DPC4 and SMAD proteins in TGF-β signalling pathways. Nature 1996;383:832–836
18 Nakao A, Afrakhte M, Moren A, Nakayama T, Christian JL, Heuchel R, Itoh S, Kawabata M, Heldin NE, Heldin CH, ten Dijke P: Identification of Smad7, a TGF-β-inducible antagonist of TGF-β signalling. Nature 1997;389:631–635.
19 Kawano K, Hirashima T, Mori S, Saitoh Y, Kurosumi M, Natori T: Spontaneous long-term hyperglycemic rat with diabetic complications, Otsuka Long-Evans Tokushima Fatty (OLETF) strain. Diabetes 1992;41:1422–1428.
20 Sato T, Asahi Y, Toide K, Nakayama N: Insulin resistance in skeletal muscle of the male Ostuka Long-Evans Tokushima Fatty rat, a new model of NIDDM. Diabetologia 1995;38: 1033–1041.
21 Ishida K, Mizuno A, Min Z, Sano T, Shima K: Which is the primary etiologic event in Otsuka Long-Evans Tokushima Fatty rats, a model of spontaneous non-insulin-dependent diabetes mellitus, insulin resistance, or impaired insulin secretion? Metabolism 1995;44:940–945.
22 Fukuzawa Y, Watanabe Y, Inaguma D, Hotta N: Evaluation of glomerular lesion and abnormal urinary findings in OLETF rats resulting from a long-term diabetic state. J Lab Clin Med 1996;128:568–578.
23 Seki N, Hashimoto N, Suzuki Y, Mori S, Amano K, Saito Y: The role of SRC homology 2-containing tyrosine phosphatase-2 on proliferation of rat smooth muscle cells. Arterioscler Thromb Vasc Biol 2002;22:1081–1085.
24 Isaka Y, Fujiwara Y, Ueda N, Kaneda Y, Kamada T, Imai E: Glomerulosclerosis induced by in vivo transfection of transforming growth factor-β or platelet-derived growth factor gene into the rat kidney. J Clin Invest 1993;92: 2597–2601.
25 Yagi K, Kim S, Wanibuchi H, Yamashita Y, Iwano H: Characteristics of diabetes, blood pressure, and cardiac and renal complications in Otsuka Long-Evans Tokushima Fatty rats. Hypertension 1997;29:728–735.
26 Kushiro M, Shikata K, Sugimoto H, Ikeda K, Horiuchi S, Makino H: Accumulation of N-σ(carboxymethyl)lysine and changes in glomerular extracellular matrix components in Otsuka Long-Evans Tokushima Fatty rats: A model of spontaneous NIDDM. Nephron 1998;79:458–468.
27 Isono M, Chen S, Hong SW, Iglesias-de la Cruz MC, Ziyadeh FN: Smad pathway is activated in the diabetic mouse kidney and Smad3 mediates TGF-β-induced fibronectin in mesangial cells. Biochem Biophys Res Commun 2002; 296:1356–1365.
28 Kleef J, Friess H, Simon P, Susmallian S, Buchler P, Zimmermann A, Büchler MW, Korc M: Overexpression of Smad2 and colocalization with TGF-β_1 in human pancreatic cancer. Dig Dis Sci 1999;44:1793–1802.
29 Tamura K, Kanzaki T, Tashiro J, Yokote K, Mori S, Ueda S, Saito Y, Morisaki N: Increased atherogenesis in Otsuka Long-Evans Tokushima Fatty rats before the onset of diabetes mellitus: Association with overexpression of PDGF β-receptors in aortic smooth muscle cells. Atherosclerosis 2000;149:351–358.
30 Mogensen CE: Microalbumiuria predicts clinical proteinuria and early mortality in maturity onset diabetes. N Engl J Med 1984;310:356–360.
31 Mattock MB, Keen H, Viberti GC, el-Gohari MR, Murrells TJ, Scott GS, Wing JR, Jackson PG: Coronary heart disease and urinary albumin excretion rate in type 2 (non-insulin-dependent) diabetic patients. Diabetologia 1998;31:82–87.
32 Mykkanen L, Zaccaro DJ, O'Leary DH, Howard G, Robbins DC, Haffner SM: Microalbuminuria and carotid artery intima-media thickness in nondiabetic and NIDDM subjects. The Insulin Resistance Atherosclerosis Study (IRAS). Stroke 1997;28:1710–1716.

Eur J Dermatol 2004; 14: 247-54

Makoto KAWASHIMA[1]
Nobukazu HAYASHI[2]
Atsuyuki IGARASHI[3]
Hirohito KITAHARA[4]
Mizue MAEGUCHI[5]
Atsuko MIZUNO[6]
Yasuko MURATA[7]
Toshitatsu NOGITA[8]
Kiyoshi TODA[9]
Ryoji TSUBOI[10]
Rie UEKI[11]
Mina YAMADA[12]
Masashi YAMAZAKI[13]
Takuma MATSUDA[14]
Yutaka NATSUMEDA[15]
Kihito TAKAHASHI[16]
Shotaro HARADA[17]

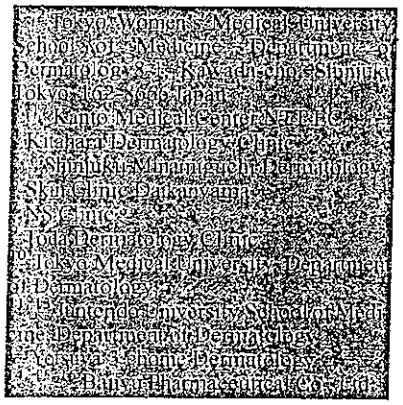

Reprints: Makoto Kawashima
Fax : (+ 81) 03 5269 7352
E-mail : m-kawash@derm.twmu.ac.jp

Article accepted on 14/05/2004
This study was supported by a grant from Banyu Pharmaceutical Co., Ltd., Tokyo, Japan.

Finasteride in the treatment of Japanese men with male pattern hair loss

Finasteride is a type 2 5α-reductase inhibitor that inhibits conversion of testosterone to dihydrotestosterone, a key mediator of male pattern hair loss (androgenetic alopecia).
The objective of this study was to identify the optimal dosage of finasteride and to evaluate its efficacy and safety in the treatment of Japanese men with male pattern hair loss. In this double- blind randomized study, 414 Japanese men with male pattern hair loss received finasteride 1 mg (n = 139), finasteride 0.2 mg (n = 137), or placebo (n = 138) once daily for 48 weeks. Efficacy was evaluated by global photographic assessment, patient self-assessment, and investigator assessment. All efficacy endpoints showed significant improvement with finasteride therapy by 12 weeks ($p < 0.05$ *versus* placebo). At 48 weeks, 58%, 54%, and 6% of men in the finasteride 1 mg, finasteride 0.2 mg, and placebo groups, respectively, had improved based on assessments of global photographs. All efficacy endpoints were numerically superior for the 1 mg dose over the 0.2 mg dose at 48 weeks. Finasteride treatment was generally well tolerated. Finasteride 1 mg/day slows hair loss and improves hair growth in Japanese men with male pattern hair loss.

Key words: androgenetic alopecia, dihydrotestosterone, finasteride, male pattern hair loss, type 2 5 α-reductase inhibitor

Male pattern hair loss, or androgenetic alopecia, is an androgen-mediated condition that is characterized by the gradual thinning of scalp hair, particularly in the frontal, temporal, and vertex regions. The incidence of this common condition increases with age and is approximately 50% among Caucasian men by the age of 50 [1-3]. Among Japanese men, the development of male pattern hair loss occurs at later ages, with an incidence at a given age similar to that among Caucasians 10 years younger [4, 5].
Hair thinning in men with androgenetic alopecia occurs secondary to the progressive miniaturization of hair follicles and shortening of the anagen (active growth) phase of the hair- growth cycle. Dihydrotestosterone is implicated as one of the principal mediators of this condition because of the fact that male pattern hair loss does not occur in men with genetic deficiency of type 2 5α-reductase, the enzyme that converts testosterone to dihydrotestosterone [6].
Finasteride is a type 2 5α-reductase inhibitor and thus inhibits the conversion of testosterone to dihydrotestosterone (DHT), lowering levels of DHT in serum and scalp [7]. Administered at 1 mg once daily, finasteride increases hair weight, promotes the conversion of hairs into the anagen phase, and can reverse hair miniaturization in men with androgenetic alopecia [8-10]. Finasteride at this dosage is generally well tolerated and has been shown to produce long-lasting improvement in scalp hair growth for up to 5 years in men with male pattern hair loss [11-13]. The objectives of this multicenter, double-blind, placebo-controlled, randomized clinical trial were to identify the optimal dosage of finasteride and to evaluate its efficacy and safety in the treatment of Japanese men with male pattern hair loss.

Methods

Patients

Patients enrolled were Japanese men, 20 to 50 years of age, with male pattern hair loss. Eligible patients were in good

Table I. *Hair growth questionnaire*

Question	Possible responses
1. Since the start of the study, I can see my bald spot getting smaller.	Strongly agree (1) → Strongly disagree (5)
2. Because of the treatment I have received since the start of the study, the appearance of my hair is :	A lot better (1) → A lot worse (7)
3. Since the start of the study, how would you describe the growth of your hair ?	Greatly increased (1) → Greatly decreased (7)
4. Since the start of the study, how effective do you think the treatment has been in slowing down your hair loss ?	Very effective (1) → Not effective at all (4)
5. Compared to the beginning of the study, which statement best describes your satisfaction with the appearance of :	
a) the hairline at the front of your head ?	Very satisfied (1) → Very dissatisfied (5)
b) the hair on top of your head ?	Very satisfied (1) → Very dissatisfied (5)
c) your hair overall ?	Very satisfied (1) → Very dissatisfied (5)

physical and mental health and had mild to moderate hair loss classified as modified Norwood-Hamilton grade II vertex, III vertex, IV, or V balding [1, 2, 4]. Patients had to agree not to change their hairstyle or use hair color throughout the study or to use other drugs for promoting hair growth.

Patients with a history of multifactorial or serious drug allergy were excluded from study participation, as were those with a history of or ongoing thyroid disease, a history of or suspected malignancy, or elevated plasma concentrations of aspartate aminotransferase (AST), alanine aminotransferase (ALT), or total bilirubin. Also excluded were patients with severe seborrheic dermatitis of the scalp and those who had undergone hair transplant surgery, scalp reduction surgery, or hair weaving.

Prior use of finasteride or any other 5 α-reductase inhibitor was cause for exclusion from the trial. The use of systemic corticosteroids or anabolic steroids, or topical corticosteroids on the area of hair loss, was not permitted during the study. Other medications were required to be withdrawn 3 to 12 months before the study and were not permitted during the study ; these included drugs known to cause hypertrichosis or hair loss as an adverse reaction (for example, zidovudine, cyclosporine, tamoxifen) for 1 year before, antiandrogenic drugs (for example, progesterone and ketoconazole) for 6 months before, minoxidil and carpronium chloride for 4 months before, and any investigational drug for 3 months before study drug administration.

The study protocol was approved by the appropriate institutional review board, and each patient signed a written consent form before participating in the study.

Study design

This 1-year, double-blind, randomized study was conducted at nine centers in Japan from June 2001 to September 2002. After the initial screening visit, patients eligible to enter the study were randomly assigned to finasteride 1 mg, 0.2 mg or placebo once daily in the morning for 48 weeks. The three types of film-coated tablets were identical in appearance. Follow-up visits were scheduled at weeks 2 and 4 and then every 4 weeks until week 48. At each visit, adverse experiences were recorded, and a medical examination was performed. Standardized clinical photographs of the head (global photographs) for clinical assessment were taken at weeks 12, 24, and 48. Patients completed a hair growth questionnaire, and investigators rated the change in hair appearance compared with baseline, at weeks 12, 24, 36, and 48.

Efficacy assessments

Global photographic assessment

The vertex and superior-frontal areas of the scalp were photographed using a standardized technique [14]. Photographs were assessed in blinded fashion by three independent dermatologists (E. Olsen, R. Savin and D. Whiting) in the United States (US) who compared the pre- and post-treatment appearance of the scalp using a 7-point scale as follows : greatly decreased (score of − 3), moderately decreased (− 2), slightly decreased (− 1), unchanged (0), slightly increased (+ 1), moderately increased (+ 2), and greatly increased (+ 3) [11]. The dermatologists in this expert panel were experienced in photographic assessments of hair growth, and this technique has been shown to have excellent reproducibility and inter-rater agreement [15].

Patient self-assessments

Every 12 weeks, patients completed a validated, self-administered hair growth questionnaire [11, 16] comprising seven questions, four relating to efficacy of treatment and three to satisfaction with appearance of scalp hair *(Table I)*. The translation of the questionnaires and the responses from English into Japanese were cross language validated by CoreMed Corp., Osaka, Japan. Responses were scored on 4 to 7 point scales, with a score of 1 assigned to the most positive response. For the statistical analysis, scores were centered on 0 (neutral response), and improvement was assigned the positive numbers.

Investigator assessments

The investigators rated change relative to baseline in hair growth in the vertex area (a global photograph of the area at baseline was used for reference), using the standardized 7 point scale described above. Investigator assessments of hair growth were made every 12 weeks after the start of study drug administration.

Safety assessments

At the screening visit, the medical history was recorded and a complete physical examination was performed. Safety assessments included physical examination and nonleading questioning about adverse experiences at each visit, as well as periodic laboratory evaluations.

Laboratory evaluations

Hematology, serum biochemical analysis, and urinalysis were performed at screening, baseline, and weeks 2, 4, 12,

Table II. *Baseline characteristics of men enrolled in the study*

	Placebo (n = 138)	Finasteride 1 mg (n = 139)	Finasteride 0.2 mg (n = 137)
Age (mean ± SD)	40 ± 6	40 ± 6	40 ± 6
No. (%) of patients with family history*	127 (92%)	122 (88%)	120 (88%)
No. (%) of patients with hair loss pattern†			
II vertex	35 (25%)	39 (28%)	43 (31%)
III vertex	40 (29%)	37 (27%)	36 (26%)
IV	44 (32%)	36 (26%)	32 (24%)
V	19 (14%)	27 (19%)	26 (19%)

** Family history = parents or siblings with history of male pattern hair loss.*
† According to modified Norwood-Hamilton scale.

24, 36, and 48. Serum prostate-specific antigen (PSA) concentrations were measured at screening and weeks 24 and 48. In addition, serum concentrations of DHT and testosterone were determined at baseline and weeks 24 and 48, while those of luteinizing hormone (LH) and follicle-stimulating hormone (FSH) were measured at baseline and 48 weeks. These assays, except DHT, were performed at the central laboratory in Japan (BML, Saitama, Japan). Serum DHT concentrations were assayed at Esoterix laboratory (Calabasas Hills, CA, USA).

Statistical analysis

Efficacy analyses were prespecified for all endpoints and were performed using the full analysis set (FAS) patient population that included all randomized patients who had a baseline and at least one post-treatment assessment. In the case of missing values, the last measured value was carried forward in the place of missing data ; data from week 24 or later were carried forward in place of missing 48-week data.

The primary efficacy endpoint was the global photographic assessment of the change in hair growth in the vertex area of the scalp at 48 weeks (final assessment) as compared with baseline. The median value of the three dermatologists' assessments was used for the global photographic endpoints score for each patient at each time point. Secondary efficacy assessments included global photographic assessment of the vertex area at weeks 12 and 24 and of the superior/frontal area at weeks 12, 24, and 48 compared with baseline, and the patient self-assessments and investigator assessment of scalp hair growth at weeks 12, 24, 36 and 48.

The presence of a dose response was tested by linear regression analysis (including study center effect) for all efficacy endpoints. Doses were log-transposed and placebo (0 mg) was assigned a value of 0.01 mg. An analysis of co variance (ANCOVA) was used for pairwise between-group comparisons (finasteride 1 mg vs placebo, finasteride 0.2 mg vs placebo, and finasteride 1 mg vs 0.2 mg). The ANCOVA model included factors for both treatment and study center. The incidence of adverse experiences and laboratory abnormalities was compared between treatment groups using Fisher's exact test.

Sample size calculations

Assuming a total of 100 patients per treatment group, we calculated that this study had approximately 90% power to demonstrate a dose response and the superiority of finasteride 1 mg over placebo as well as the superiority of finasteride 0.2 mg over placebo. This calculation was based on data from a previous 24-week study (phase II dose range study [17]) to estimate the following scores for the primary endpoint (global photographic assessment scores for the vertex area at 48 weeks) : finasteride 1 mg group, 0.647 ; finasteride 0.2 mg group, 0.427 ; placebo group, 0.010. The current study randomized approximately 125 patients per treatment group to account for a projected discontinuation rate of 20%.

Results

Baseline patient demographics and accounting

A total of 414 patients were enrolled in the study. Baseline characteristics of enrolled patients were not significantly different among the three treatment groups and are summarized in *Table II.* The mean age of enrolled patients was 40 years, and most (89-92%) had a family history of hair loss.

Patient accounting is summarized in *Fig. 1.* All patients were included in the safety analyses, and one patient in the finasteride 0.2 mg treatment group was excluded in all FAS efficacy analyses because of ineligibility (hair weaves) for study.

Global photographic assessment

At 48 weeks, over half of the patients in the two finasteride treatment groups demonstrated improvement relative to baseline in global photographic assessment of the vertex area *(Fig. 2).* Rates of improvement (vertex scalp hair slightly, moderately, or greatly increased) in hair growth relative to baseline were 58%, 54%, and 6% in the finasteride 1 mg, finasteride 0.2 mg, and placebo groups, respectively, whereas rates of deterioration (vertex scalp hair slightly, moderately, or greatly decreased) in hair growth relative to baseline were 2%, 5%, and 22%, respectively. The mean scores at 48 weeks *(Fig. 3A)* demonstrated a significant dose response ($p < 0.001$). Moreover, the mean score for each of the finasteride treatment groups was significantly better ($p < 0.001$) than that for the placebo group. Although the study was not designed to detect a significant difference between the two finasteride doses, the mean score (mean ± standard error) for the 1 mg finasteride group (0.7 ± 0.1) was numerically but not significantly superior to that for the 0.2 mg group (0.6 ± 0.1). Scores were similar for patients with different grades of hair loss at baseline (data not shown).

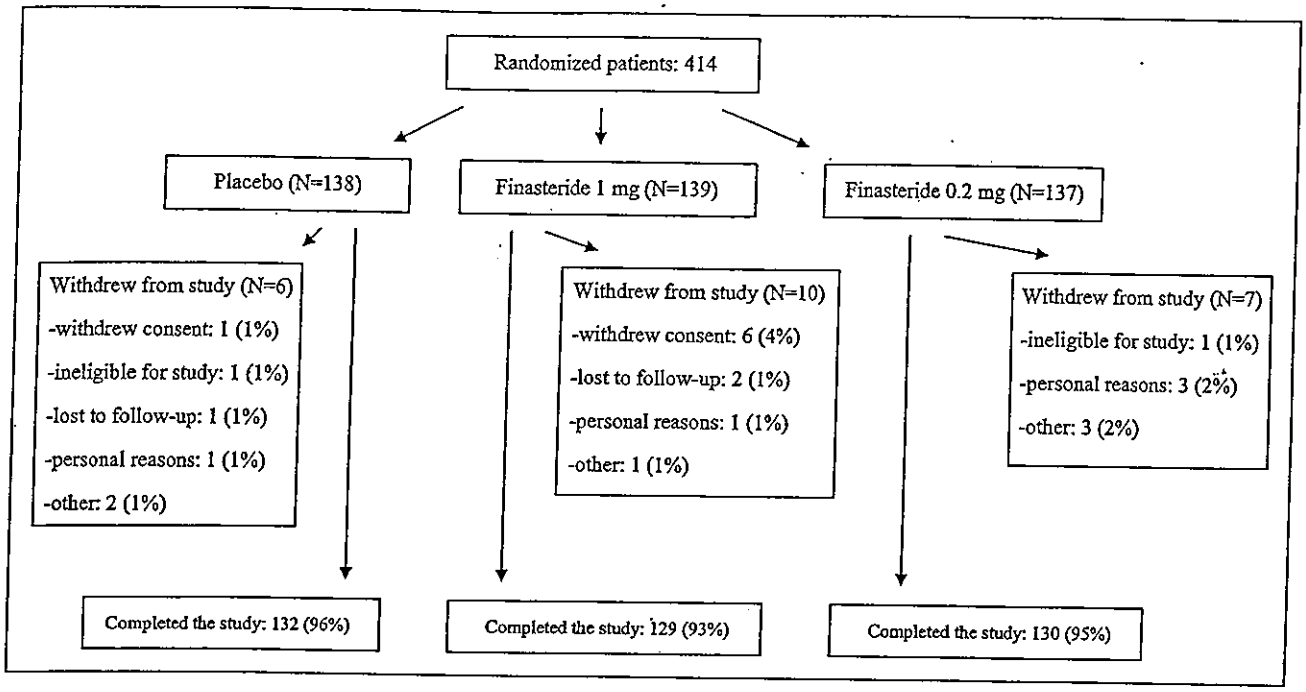

Figure 1. *Patient accounting.*

Vertex global photographic assessment scores for finasteride-treated patients showed improvement at 12 and 24 weeks and then remained stable, while those for patients in the placebo group gradually declined *(see Fig. 3A)*. These scores were significantly better for the finasteride groups compared with the placebo group ($p < 0.001$), and a statistically significant dose response ($p < 0.001$) was evident at 12 and 24 weeks.

Global photographic assessment scores for the superior-frontal view are depicted in *Fig. 3B*. As with the vertex view, scores for the superior-frontal view increased in the finasteride groups at both 12 and 24 weeks and then remained stable, while scores for the placebo group declined. Scores for both finasteride groups were significantly better

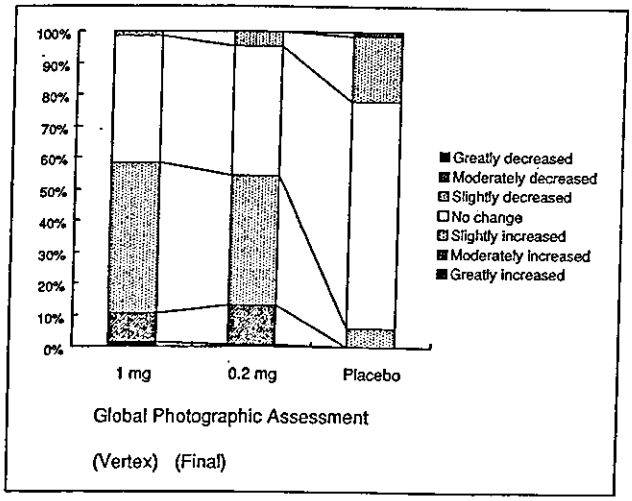

Figure 2. *Global photographic assessment of hair growth on the vertex area of the scalp, compared with baseline, after 48 weeks of treatment with finasteride 1 mg, finasteride 0.2 mg, or placebo once daily.*

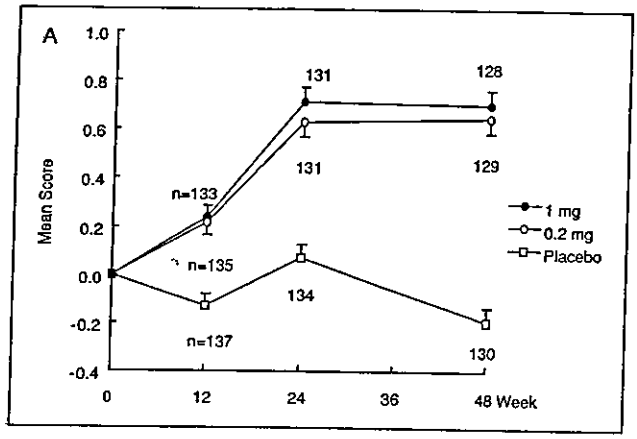

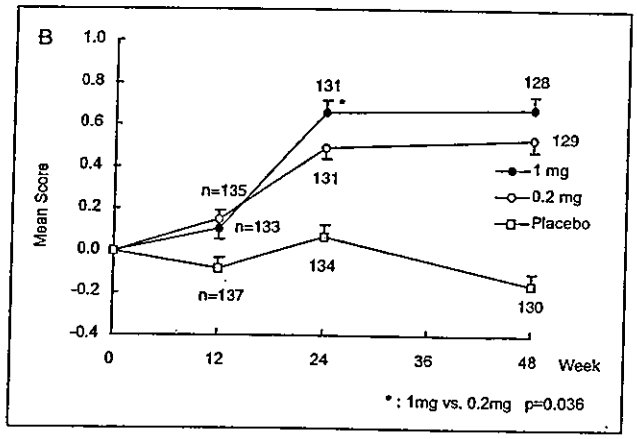

Figure 3. *Mean (± SE) global photographic assessment score for the vertex area (A) and superior-frontal area (B) of the scalp during 48 weeks of treatment (FAS population). $P < 0.001$ for the comparison between each finasteride treatment group and placebo at 12, 24, and 48 weeks. n in Fig means the number of statistically analyzed patients.*

($p \leq 0.006$) than that for the placebo group, and a significant dose response ($p \leq 0.002$) was evident at each time point. Representative global photographs of patients rated by the expert panel as having decreased or increased hair growth at 24 and 48 weeks are shown in *Fig. 4*.

Patient self-assessment

The mean scores for all seven patient self-assessment questions were significantly better for each of the finasteride treatment groups compared with the placebo group at each time point beginning at 12 weeks ($p \leq 0.007$ for all finasteride-placebo comparisons). Moreover, a significant dose response ($p \leq 0.003$) was found at each time point for each question. At 48 weeks, scores for the finasteride 1 mg group were numerically superior to those for the finasteride 0.2 mg group for each question.

A greater percentage of finasteride- than placebo-treated patients reported an improvement in each question at each time point. The proportion of men reporting improvement from baseline at Week 48 is depicted in *Fig. 5*.

Investigator assessment

The investigator assessment scores were significantly better for both the finasteride 1 mg ($p \leq 0.004$) and finasteride 0.2 mg ($p \leq 0.024$) groups compared with the placebo group at each time point from 12 weeks onward *(Fig. 6)*. Moreover, a significant ($p \leq 0.002$) dose response was found for each time point. At 48 weeks, investigators rated 60%, 61%, and 19% of patients in the finasteride 1 mg, finasteride 0.2 mg and placebo groups, respectively, as having improved.

Serum hormone and prostate-specific antigen concentrations

Pretreatment serum hormone and PSA concentrations were similar in the three treatment groups. Mean serum concentrations of DHT fell in the finasteride 0.2 and 1 mg groups from baseline concentrations. The percent change in DHT concentration was significantly larger ($p < 0.001$) in each of the finasteride groups compared with the placebo group. Serum testosterone concentrations increased in the finasteride 0.2 and 1 mg groups. Although the percent increases in serum testosterone at 48 weeks were significantly greater ($p = 0.014$ and $p = 0.028$, respectively) in the finasteride groups compared with the placebo group, serum concentrations of testosterone remained well within the normal range. Differences between the two finasteride groups were not significant for changes in serum DHT or testosterone concentrations.

There were no statistically significant differences between the finasteride and placebo groups in changes in LH or FSH concentrations during the study.

Pretreatment serum concentrations of PSA were 0.9 ng/ml in both finasteride treatment groups and 1.0 ng/ml in the placebo group (reference range, ≤ 4.0 ng/ml). As expected, the administration of finasteride was associated with a small decrease in serum PSA concentrations from baseline in the finasteride 1 mg group (– 0.3 ng/ml) and 0.2 mg group (– 0.2 ng/ml). There was no significant difference in the change in PSA level between the two finasteride groups.

Adverse experiences

There were no deaths or serious drug related adverse experiences and no drug related adverse experiences which resulted in discontinuation of the study medication during the trial. The incidence of drug related adverse experiences was not significantly different between groups (5%, 1.5% and 2.2% for the finasteride 1 mg, 0.2 mg and placebo groups, respectively, $p \geq 0.173$) ; of these, adverse experiences related to sexual function, particularly decreased libido, were most commonly reported (incidence of 2.9%, 1.5%, and 2.2%, respectively), and most resolved without discontinuation of therapy. These adverse experiences related to sexual function reported in the study were mild in intensity.

There were no significant differences between treatment groups in the overall incidence of laboratory abnormalities (16%, 12%, and 10%, respectively ; $p \geq 0.148$). The only abnormalities considered possibly related to treatment by the investigator were a mild increase in total cholesterol and a mild increase in ALT in two patients in the 1 mg finasteride group ; neither was considered to be clinically significant.

Discussion

We found that once daily treatment with finasteride at a dose of 0.2 or 1 mg for 48 weeks was effective in improving the appearance of scalp hair and slowing the loss of hair in Japanese men with male pattern hair loss. Significant improvement in hair growth with finasteride therapy relative to placebo was evident as early as 12 weeks for all measured endpoints. At 48 weeks, global photographs showed improvement from baseline for 58% of patients in the finasteride 1 mg group, while deterioration was recorded for only 2% of patients. These findings agree with those of previous US and multinational, non-Asian studies enrolling predominantly Caucasian men aged 18 to 41 years with male pattern hair loss [11, 17, 13].

Both finasteride doses were significantly more effective than placebo. Although the study was not designed to detect a significant difference between the two finasteride doses, a significant dose response was found, and the results for the 1 mg dose were significantly better than those for the 0.2 mg dose for some of the secondary endpoints. These data were well agreed with those in previous US study [17]. Moreover, at 48 weeks, all efficacy endpoints were numerically superior for the 1 mg dose. Thus, from the standpoint of efficacy, 1 mg appears to be the optimal dose for Japanese men with male pattern hair loss.

The 1 mg dose was selected as the optimal dose in prior non-Japanese, dose- ranging studies and is the dose marketed in over 60 countries for treatment of male pattern hair loss. Results of pharmacokinetic studies in healthy volunteers indicate that the pharmacokinetics of finasteride, as well as the effect of finasteride in lowering DHT concentrations, are similar in Japanese and non-Japanese male subjects (data on file, Banyu Pharmaceutical Co, Ltd, Tokyo, Japan). The findings of this study suggest that the beneficial clinical effects of finasteride are also similar in Japanese and non-Japanese men. Moreover, results of two recent open-label studies indicate that therapy with finasteride may be effective also for treating Taiwanese and Indian men with male pattern hair loss [18, 19].

The incidence of male pattern hair loss increases with age in both Japanese and Caucasian men ; however, the onset of male pattern hair loss occurs at later ages among Japanese men. The incidence of male pattern hair loss in Japanese